

Approximating Multiplicatively Weighted Voronoi Diagrams: Efficient Construction with Linear Size

Joachim Gudmundsson  

University of Sydney, Australia

Martin P. Seybold  

University of Vienna, Faculty of Computer Science, Theory and Applications of Algorithms,
Währinger Straße 29, A-1090 Vienna, Austria

Sampson Wong  

University of Copenhagen, Copenhagen

1 Abstract

Given a set of n sites from \mathbb{R}^d , each having some positive weight factor, the Multiplicatively Weighted Voronoi Diagram is a subdivision of space that associates each cell to the site whose weighted Euclidean distance is minimal for all points in the cell.

We give novel approximation algorithms that output a cube-based subdivision such that the weighted distance of a point with respect to the associated site is at most $(1 + \varepsilon)$ times the minimum weighted distance, for any fixed parameter $\varepsilon \in (0, 1)$. The diagram size is $O_d(n \log(1/\varepsilon)/\varepsilon^{d-1})$ and the construction time is within an $O_D(\log(n)/\varepsilon^{(d+5)/2})$ -factor of the size bound. We also prove a matching lower bound for the size, showing that the proposed method is the first to achieve *optimal size*, up to $\Theta(1)^d$ -factors. In particular, the obscure $\log(1/\varepsilon)$ factor is unavoidable. As a by-product, we obtain a factor $d^{O(d)}$ improvement in size for the unweighted case and $O(d \log(n) + d^2 \log(1/\varepsilon))$ point-location time in the subdivision, improving the known query bound by one d -factor.

The key ingredients of our approximation algorithms are the study of convex regions that we call cores, an adaptive refinement algorithm to obtain optimal size, and a novel notion of *bisector coresets*, which may be of independent interest. In particular, we show that coresets with $O_d(1/\varepsilon^{(d+3)/2})$ worst-case size can be computed in near-linear time.

2012 ACM Subject Classification Theory of computation \rightarrow Computational geometry

Keywords and phrases Multiplicatively Weighted Voronoi Diagram, Compressed QuadTree, Adaptive Refinement, Bisector Coresets, Semi-Separated Pair Decomposition, Lower Bound

Related Version See <https://arxiv.org/abs/2112.12350> for the full version of the paper.

Acknowledgements This work was supported under the Australian Research Council Discovery Projects funding scheme (project number DP180102870) and partially supported by Starting Grant 1054-00032B from the Independent Research Fund Denmark under the Sapere Aude research career programme. This project has received funding from the European Research Council (ERC) under the European Union's Horizon 2020 research and innovation programme (Grant agreement No. 101019564) and the Austrian Science Fund (FWF) project Z 422-N, project I 5982-N, and project P 33775-N, with additional funding from the *netidee SCIENCE Stiftung*, 2020–2024.



17 **1** Introduction

Voronoi Diagrams are structures of fundamental importance for many scientific fields. In particular, planar variants with linear worst-case size are very well understood (e.g. [8, 10]). Though closely related to the Nearest-Neighbor search problem, the *explicit* subdivisions provided by Voronoi Diagrams are a central tool for various problems, including meshing in scientific computing, planning of facility locations, motion planning, or surface reconstruction.

Given a set of sites $\{s_1, \dots, s_n\} \subset \mathbb{R}^d$, each having a positive weight $w_i > 0$, their Multiplicatively Weighted Voronoi Diagram (MWVD) is the subdivision of \mathbb{R}^d into cells that



© Joachim Gudmundsson, Martin P. Seybold and Sampson Wong;
licensed under Creative Commons License CC-BY 4.0

40th International Symposium on Computational Geometry (SoCG 2024).

Editors: Wolfgang Mulzer and Jeff M. Phillips; Article No. XX; pp. XX:1–XX:14



Leibniz International Proceedings in Informatics

Schloss Dagstuhl – Leibniz-Zentrum für Informatik, Dagstuhl Publishing, Germany



XX:2 Approximate Multiplicatively Weighted Voronoi Diagrams with Optimal Size

25 associates each cell to one site, i.e. the site s_i that minimizes $\|p - s_i\|_2/w_i$ for all points p in
26 the cell. Though all bisectors in an MWVD are either half-spaces ($w_i = w_j$) or Apollonian
27 spheres ($w_i \neq w_j$), the two main difficulties with MWVDs are that Voronoi regions may
28 contain holes, and that the multiplicative weights can violate the triangle inequality.

29 The MWVD in \mathbb{R}^1 has linear size and can be obtained using a Divide & Conquer algorithm
30 in $O(n \log n)$ time [6]. Aurenhammer and Edelsbrunner showed that MWVDs in \mathbb{R}^2 can
31 have $\Omega(n^2)$ size and gave a worst-case optimal algorithm [7]. Held and de Lorenzo [17] gave
32 a sweep approach for 2D that runs in $O(n^2 \log n)$ time. In special cases, 2D MWVD size is
33 known to have near-linear, or even linear, bounds [16, 11]. In general, unweighted Voronoi
34 Diagrams, i.e. all $w_i = 1$, are well known to have $\Omega(n^{\lceil d/2 \rceil})$ worst-case size (see e.g. [13]).

35 **Importance of cube-based Approximate Voronoi Diagrams.** We limit our discussion on
36 two applications where the simplicity of cube-based AVDs is key for strong bounds.

37 (i) Axis-Aligned Segment-Queries in 2D.

38 Using Chazelle’s Point-Location & Walk method [9, Sect. 4.2] on an 2D MWVD, it
39 is possible to traverse all k cells of the subdivision that are intersected by an axis-
40 aligned query line-segment in $O(\log(n) + k)$ time, which determines the $\Omega(k)$ distinct
41 nearest-sites for (the sequence of points that are contained in) the query-segment.

42 Now, an approximate subdivision that consists of canonical squares, or set difference of
43 canonical squares, allows to merge common boundaries of adjacent squares, associated
44 to the same Voronoi site, without increasing the size bound of the subdivision. Thus,
45 allowing to retain the $O(\log(n) + k)$ query bound in the approximate setting.

46 (ii) **Fast Point-Queries when d is large.** The ‘curse of dimensionality’ typically refers
47 to the broad phenomena that either the query-bounds or the space-bounds of known
48 structures for (exact) nearest-neighbor search deteriorate ‘quickly’ as d increases. In
49 ε -approximate nearest-neighbor search, we are mainly interested in the range $d = 2$ to
50 $d = O(\log(n)/\varepsilon^2)$, due to Johnson-Lindenstrauss dimension reduction (see, e.g., [13, 14]).
51 Now, cube-based subdivisions allow to use compressed QuadTrees to obtain *very strong*
52 query bounds. For example, in a subdivision of \mathbb{R}^d with $N = O(n/\varepsilon^d)$ cubes, the query
53 time is $O(d \log(n/\varepsilon^d)) = O(d \log(n) + d^2 \log(1/\varepsilon))$.

54 In contrast, query bounds containing $O(1)^d$ -terms are only fast when d is *very small*.

55 For careful comparison with respect to the dimension, we distinguish between O -notation,
56 O_D -notation that assumes a ‘constant-dimension’ and hides $d^{O(d)}$ -factors, and O_d -notation
57 that assumes a ‘small-dimension’ and hides $O(1)^d$ -factors. E.g. $O((8d)^d) = O_d(d^d) = O_D(1)$.
58 Note that there is a separation between space bounds in the O_D -regime and the O_d -regime.
59 For $d = O(\log \log n)$, any $O(1)^d$ factors in size are $O(\text{polylog } n)$ factors, whereas d^d -factors
60 are $\omega(\text{polylog } n)$. Further, c^d -factors in size are sub-linear $O(n^{1/p})$ for $d \leq \log_c(n)/p$, unlike
61 d^d -factors.

62 This work studies the problem of computing ε -Approximate MWVDs for prescribed
63 $\varepsilon > 0$. That is, a subdivision of \mathbb{R}^d into cells that are cubes, or set-difference of cubes, that
64 associates each cell with one site that is an ε -approximate weighted nearest-neighbor for all
65 points in the cell. The only known solution til date is to employ the, more general, framework
66 of Har-Peled and Kumar [15], which, e.g., found application in the work [3].

67 **Contribution and Paper Organization.** Our approach considers convex regions that we call
68 ‘cores’, which are the intersection of at most $n - 1$ Apollonian balls of MWVD bisectors. In
69 Section 3, we introduce an Adaptive Refinement algorithm that ε -approximates each core with

Diagram	Technique	Size	Runtime
ε -AVD	Clustering, PLEB [12]	$O_D\left(n \frac{\log n}{\varepsilon^d} \log \frac{n}{\varepsilon}\right)$	$\times O_D\left(\log \frac{n}{\varepsilon}\right)$
ε -AVD	Clustering, ε -PLSB [18]	$O_D\left(n \frac{\log 1/\varepsilon}{\varepsilon^{d+1}}\right)$	$\times O_D\left(\log \frac{n}{\varepsilon}\right)$
ε -AVD	Triangle ineq., 8-WSPD [4, p148]	$O_d\left(n \left(\frac{d}{\varepsilon}\right)^d \log \frac{1}{\varepsilon}\right)$	$\times O_D\left(\frac{1}{\varepsilon^d} \log \frac{n}{\varepsilon}\right)$
$(1, \varepsilon)$ -AVD	Triangle ineq. [5, Cor. 9.10.f]	$O_D\left(\left(n/\varepsilon^{d-1}\right) \log \frac{1}{\varepsilon}\right)$	
ε -AMWVD	Clustering, Sketches [15]	$O_D\left(n \left(\frac{\log^{d+2}(n)}{\varepsilon^{2d+2}} + \frac{1}{\varepsilon^{d(d+1)}}\right)\right)$	
ε -AMWVD	Adaptive Refinement, ε^{-1} -SSPD	$\Theta_d\left(n \frac{\log 1/\varepsilon}{\varepsilon^{d-1}}\right)$	$\times O_D\left(\frac{\log n}{\varepsilon^{(d+5)/2}}\right)$

95 **Table 1** Overview of constructions of ε -AVDs that provide *fast queries* for large d and the proposed
 96 method for ε -AMWVDs. Note that ε -AMWVDs are more general than the unweighted ε -AVDs. The
 97 time bound of [15] is $O_D(n \log^{2d+3}(n)/\varepsilon^{2d+2} + n/\varepsilon^{d(d+1)})$, and the query time $O(d \log(n/\varepsilon^{d(d+1)}))$
 98 is *cubic* in d . All other QuadTree based ε -AVD methods have $O(d \log(n/\varepsilon^d))$ query time.

70 a set of d -cubes, and show that each core is ε -approximated with $O_d(\log(1/\varepsilon)/\varepsilon^{d-1})$ cubes.
 71 In Section 3.1, we show that a top-down propagation in the compressed QuadTree over the
 72 set of d -cubes allows to obtain an ε -AMWVD that consists of $O_d(n \log(1/\varepsilon)/\varepsilon^{d-1})$ cells that
 73 are d -cubes, or the set difference of d -cubes, each of which associated to *one site* that is
 74 weighted nearest-neighbor for all points in the cell, up to a $(1 + \varepsilon)$ factor. One by-product of
 75 our construction is thus a compressed QuadTree that can report an ε -NN of a query-point in
 76 $O(d \log(n) + d^2 \log(1/\varepsilon))$ time, thus improving on the query-time of the structure from [15]
 77 by one d -factor.

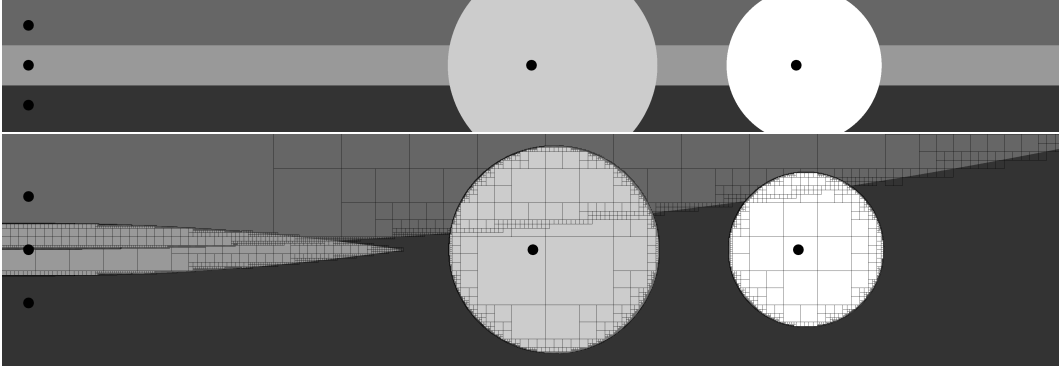
78 We prove a matching lower bound on the size of the subdivision in Section 4. Specifically,
 79 we show that *every* subdivision of \mathbb{R}^d , formed by axis-aligned hyper-rectangles, that is an
 80 ε -approximation of an Apollonian ball must contain $\Omega_d(\log(1/\varepsilon)/\varepsilon^{d-1})$ hyper-rectangles. Our
 81 proposed bound improves on the known $\Omega_d(\varepsilon/(\varepsilon\sqrt{d})^d)$ bound from [4, 5] in two ways. First,
 82 the denominator is free of the \sqrt{d} -factor and, second, it is the first known lower bound that
 83 shows that a $\log(1/\varepsilon)$ -factor is *required* in the space. Thus, the proposed construction is the
 84 first that computes an ε -AMWVD with worst-case optimal size, up to $\Theta_d(1)$ -factors.

85 In Section 5, we introduce our second approximation algorithm which is the key component
 86 to improve the construction time from quadratic to near-linear. We show that cores admit
 87 an ε -approximation with low complexity, i.e. with $O_d(1/\varepsilon^{(d+3)/2})$ bisectors, and give an
 88 algorithm that outputs such bisector coresets in $O_D(n \log(n)/\varepsilon^{3(d+1)/2})$ time, based on an
 89 $O(1/\varepsilon)$ -Semi-Separated Pair Decomposition (SSPD) of the site locations. If the sites are
 90 a point set with polynomially bounded spread, the construction time improves from an
 91 O_D -bound to the respective O_d -bound.

92 See Table 1 for an overview of the size and runtime of known ε -AVD constructions, and
 93 our proposed method. Due to the large amount of previous work, we only include those
 94 methods that also compute cube-based Approximate Voronoi Diagrams in the comparison.

99 **2 Preliminaries**

100 We provide a brief overview of canonical d -cubes and QuadTrees. The *canonical cube system*
 101 is an hierarchical and infinite tiling of \mathbb{R}^d with canonical cubes. Level zero of the canonical
 102 cube system consists of unit cubes with vertices at integer coordinates. For all $\ell \leq -1$, we



127 **Figure 1** The top shows an example of an exact MWVD of five sites ($\varepsilon_S = 0$). The bottom shows
 128 an ε_S -AMWVD of the same instance obtained from cores with $\varepsilon_S = 0.01$. Result squares of the
 129 proposed Adaptive Refinement algorithm (Section 3) for all four cores are shown as black overlay.

103 construct level ℓ by bisecting each cube in level $\ell + 1$ along each of the d axes. Therefore, there
 104 are 2^d cubes in level ℓ per cube in level $\ell + 1$. For all $\ell \geq 1$, we merge 2^d cubes in level $\ell - 1$ to
 105 obtain a single cube in level ℓ , so that the cubes in level ℓ form a tiling of \mathbb{R}^d . For example, a
 106 d -cube is a subset of points from \mathbb{R}^d of the form $[2^\ell x_1, 2^\ell(x_1 + 1)] \times \dots \times [2^\ell x_d, 2^\ell(x_d + 1)]$ for
 107 integers ℓ, x_1, \dots, x_d . Note that any two d -cubes from the system are either interior disjoint
 108 or one cube is a subset of the other.

109 Given a set of n canonical d -cubes from the system, one can build a QuadTree on the set
 110 of cubes, in $O(dn \log \Delta)$ time, where Δ is the ratio between longest and shortest side length
 111 of the input set. In this work, we use compressed QuadTrees, which have $O(dn)$ size and can
 112 be constructed in $O(dn \log n)$ time. The subdivision of \mathbb{R}^d induced by a QuadTree consists
 113 of canonical d -cubes, whereas the subdivision induced by a compressed QuadTree consists of
 114 regions that are the set difference of canonical d -cubes.

115 2.1 Voronoi Maps, Apollonian Balls, and the Core

116 Mapping $\lambda : \mathbb{R}^d \rightarrow \{1, \dots, n\}$ is called a Voronoi Map for the distance functions $\{d_1, \dots, d_n\}$,
 117 if $d_{\lambda(x)}(x) \leq \min_i d_i(x)$, for all points $x \in \mathbb{R}^d$. The d_i with index $i = \lambda(x)$ is called a
 118 nearest-neighbor of point x . In the case of Multiplicatively Weighted Voronoi Diagrams,
 119 each site $s_i \in \mathbb{R}^d$ has a positive weight-factor w_i and the distance is $d_i(x) = \|x - s_i\|/w_i$.
 120 We denote by $\|\cdot\|$ the Euclidean ℓ_2 -norm and indicate other ℓ_p -norms explicitly by $\|\cdot\|_p$.
 121 A subdivision of \mathbb{R}^d is called MWVD if every cell in the subdivision is associated to one
 122 input site, and if mapping the points in a cell to the associated site is a Voronoi Map. Cell
 123 boundaries occur where the weighted distances to two sites are equal, which is along an
 124 Apollonian circle for $d = 2$. For general d , we define the Apollonian sphere between s_i
 125 and s_j to be $\{x \in \mathbb{R}^d : \|x - s_i\|/w_i = \|x - s_j\|/w_j\}$. A trivial MWVD is to construct the
 126 arrangement of the $\binom{n}{2}$ Apollonian spheres, giving a polynomial size bound.

130 **Approximate Voronoi Maps of Apollonian Spheres and cube-based ε -AVDs** A mapping
 131 $\lambda : \mathbb{R}^d \rightarrow \{1, \dots, n\}$ is called an ε -approximate Voronoi Map for the functions $\{d_1, \dots, d_n\}$,
 132 if $d_{\lambda(x)}(x) \leq (1 + \varepsilon) \min_i d_i(x)$, for all points $x \in \mathbb{R}^d$.

133 Recall that the MWVD bisector of s_j and s_i is a $(d - 1)$ -dimensional hyper-plane, if
 134 $w_j = w_i$. We introduce a parameter $\varepsilon_S \in [0, \varepsilon]$, that we calibrate in Section 5.2, and use it
 135 to ε_S -approximate hyper-planes with hyper-spheres. (This will turn out advantageous for

136 obtaining optimal size.) Let the sites be sorted by weight, so that $w_1 \leq \dots \leq w_n$, breaking
 137 ties arbitrary but *fixed*. We define for all indices $i < j$ the Apollonian balls

$$138 \quad \text{ball}(i, j) = \text{ball}(s_i, s_j, \gamma_{ij}) = \{x \in \mathbb{R}^d : \|x - s_i\| \gamma_{ij} \leq \|x - s_j\|\} , \quad (1)$$

139 where $\gamma_{ij} := \max(w_j/w_i, 1 + \varepsilon_S)$. We call γ_{ij} the *effective weight* of $\text{ball}(i, j)$. For $\varepsilon_S > 0$,
 140 $\gamma_{ij} \geq 1 + \varepsilon_S$ and it follows that $\text{ball}(i, j)$ is not a half-space. Note that the arrangement of
 141 the surfaces of all $\{\text{ball}(i, j)\}$ yields an ε_S -approximate Voronoi Map. See [Figure 1](#).

142 To enable *fast* point location with Compressed Quad-Trees, an ε -Approximate Voronoi
 143 Diagram (ε -AVD) is a subdivision of \mathbb{R}^d into d -cubes, and set-difference of d -cubes, that is
 144 an ε -approximate Voronoi Map. That is, each cube in the subdivision of \mathbb{R}^d is associated to
 145 *one* input site that is an ε -Nearest-Neighbor for all points in the cube.

146 **Closest, Furthest, and the Core of Apollonian Balls** We further define $t^*(s_i, s_j, \gamma_{ij})$ to be
 147 the *closest distance* from s_i to a point on the surface of $\text{ball}(i, j)$, and $t^\dagger(s_i, s_j, \gamma_{ij})$ to be the
 148 *furthest distance* from s_i to a point on the surface of $\text{ball}(i, j)$. Note that these points are on
 149 the line through s_i and s_j , and their distances are

$$150 \quad \gamma_{ij} = \max(w_j/w_i, 1 + \varepsilon_S) \quad (2)$$

$$151 \quad t_{ij}^* = t^*(s_i, s_j, \gamma_{ij}) = \|s_j - s_i\| / (\gamma_{ij} + 1) \quad (3)$$

$$152 \quad t_{ij}^\dagger = t^\dagger(s_i, s_j, \gamma_{ij}) = \|s_j - s_i\| / (\gamma_{ij} - 1) . \quad (4)$$

153 For example, $\text{ball}(i, j)$ has diameter $t_{ij}^* + t_{ij}^\dagger$.

154 Let the set of balls of site s_i be $B_i := \{(i, j) : i < j\}$. For every subset $A_i \subseteq B_i$, define
 155 the convex region $\text{core}(A_i) := \bigcap_{(i, j) \in A_i} \text{ball}(i, j)$. By definition, the point $s_i \in \text{core}(A_i)$ for
 156 all non-empty $A_i \subseteq B_i$.

157 **3 Small Approximate Voronoi Diagrams using $\binom{n}{2}$ Bisectors**

158 The exact Voronoi region of site s_j in an MWVD is $\text{core}(B_j) \setminus \bigcup_{i < j} \text{core}(B_i)$ and a simple
 159 construction of the Voronoi Map may process the regions $\text{core}(B_j)$ by descending index j
 160 and assign all points in $\text{core}(B_j)$ to the index j . We introduce a suitable discretization for
 161 this idea next.

162 **► Lemma 1.** *There exist two balls centered at s_i , one with radius R containing $\text{core}(B_i)$,
 163 and one with radius r contained in $\text{core}(B_i)$, so that $R/r \leq 3/\varepsilon_S$. I.e. $\text{core}(B_i)$ is $3/\varepsilon_S$ -fat.*

164 **Proof.** Since any bisector has $t_{ij}^\dagger/t_{ij}^* = \frac{\gamma_{ij}+1}{\gamma_{ij}-1} \leq 1 + 2/\varepsilon_S$ and the intersection of bisectors
 165 retains the maximum over those ratios, $\text{core}(B_i)$ is $3/\varepsilon_S$ -fat with $r := \min_j \{t_{ij}^*\}$. ◀

166 To discretize a $\frac{R}{r}$ -fat region for some $\varepsilon_A \in (0, \varepsilon_S)$, we consider the coarsest level where the
 167 canonical cubes have diameter at most $\text{diam}(C) \leq r\varepsilon_A$, i.e. side-length $\text{len}(C) \leq r\varepsilon_A/\sqrt{d}$.
 168 Within distance at most R from s_i , there are $O_d((\frac{2R}{r} \cdot \frac{\sqrt{d}}{\varepsilon_A})^d) = O_d((\sqrt{d}/\varepsilon_A^2)^d)$ such cubes.
 169 Checking each of the k bisectors that define the fat region, we can determine with $O(k)$
 170 distance computations if the centroid point of a cube is in $\text{core}(B_i)$. Since any one cube is
 171 entirely inside, is entirely outside, or contains a point of the boundary, we have that only
 172 the latter case is potentially incorrect when deciding membership by the cube's centroid
 173 point. Since any point x on the boundary has $\|x - s_i\| \geq r$ and any point q with erroneous

XX:6 Approximate Multiplicatively Weighted Voronoi Diagrams with Optimal Size

174 membership decision has $\|q - x\| \leq \varepsilon_A r$ from a point x on the boundary (i.e. $d_i(x) = d_j(x)$),
 175 the discretization of the core approximates within a factor

$$\begin{aligned}
 176 \quad \frac{d_i(q)}{d_j(q)} &= \frac{d_i(q)}{d_i(x)} \cdot \frac{d_i(x)}{d_j(q)} \leq \left(1 + \frac{\|x - q\|}{\|x - s_i\|}\right) \frac{d_j(x)}{d_j(q)} \leq \left(1 + \frac{\|x - q\|}{\|x - s_i\|}\right) \left(1 + \frac{\|x - q\|}{\|q - s_j\|}\right) \\
 177 \quad &\leq (1 + \varepsilon_A) \left(1 + \frac{\varepsilon_A r}{\|q - s_j\|}\right) \leq (1 + \varepsilon_A) \left(1 + \frac{\varepsilon_A r}{\|x - s_j\| - \|x - q\|}\right) \\
 178 \quad &\leq (1 + \varepsilon_A) \left(1 + \frac{\varepsilon_A r}{\|x - s_i\| - \|x - q\|}\right) \leq (1 + \varepsilon_A) \left(1 + \frac{\varepsilon_A}{1 - \varepsilon_A}\right) = 1 + O(\varepsilon_A) .
 \end{aligned}$$

179 ► **Observation 2.** $O(1/\varepsilon)$ -fat cores allow a discretization of $O_d(n(\sqrt{d}/\varepsilon^2)^d)$ total size that
 180 ε -approximates each core. Construction time is at most a factor $d \cdot n$ over the size bound.

181 Note that the argument for cubes that intersect the boundary in our approximation
 182 bound already holds if the maximum distance of two points in a cube (diameter) is sufficiently
 183 small with respect to the distance to s_i , and not just if the diameter is at most $r\varepsilon_A$. Next,
 184 we discuss our, more space efficient, top-down search method that exploits this fact. (Note
 185 that $O(\log(1/\varepsilon_S))$ levels of the canonical cube system are relevant for any given core.)

186 As such, our Adaptive Refinement algorithm first determines $r = \min\{t_{ij}^*\}$ from the given
 187 set of k bisectors of site s_i , and then starts on the smallest canonical cube that contains the
 188 ball of radius $3r/\varepsilon_S$ around the site s_i . Recursively, we check if the current cube C is entirely
 189 inside or entirely outside, i.e. $\|centr(C) - centr(ball(i, j))\| + diam(C)/2 \leq rad(ball(i, j))$
 190 for all $j > i$ or $\|centr(C) - centr(ball(i, j))\| - diam(C)/2 > rad(ball(i, j))$ for a $j > i$. If so,
 191 the search stops and includes the current cube C in the result set, or respectively excludes
 192 it. Otherwise, we check if the cube's diameter is sufficiently small for the centroid-test, i.e.
 193 $diam(C) \leq \varepsilon_A (\|s_i - centr(C)\| - diam(C)/2)$. If not, then all 2^d children of the cube are
 194 searched recursively. If it is, then we stop the search and include the cube in the output set
 195 based on the result of its centroid-test, i.e. cube C is included if and only if the centroid
 196 point of C is inside *each* of the k bisectors that define $core(B_i)$.

197 Note that the search stops descending on a cube C if one of the two criteria holds.
 198 Termination and correctness follow immediately from the above discussion. To improve on
 199 the above size bound, we bound the total number of canonical cubes that the search visits,
 200 each of which taking $O(d \cdot k)$ time.

201 ► **Definition 3** (Distance Classes). Let $ball_s(x) = \{p : \|s - p\| \leq x\}$ be the ball of radius
 202 x around site s . Let L be the set of canonical cubes that our top-down search, **Adaptive**
 203 **Refinement**, visits. We partition $L =: \bigcup_j L_j$ in distance classes, such that L_j contains those
 204 cubes $C \in L$ where $C \subseteq ball_s(2^j r)$ and $C \not\subseteq ball_s(2^{j-1} r)$.

205 Note that $L_j = \emptyset$ for $j \leq -2$, since such a cube C would be contained in $ball_s(r/4)$.
 206 Consequently, its parent C' would be contained in $ball_s(r/2)$, satisfying the inclusion-test
 207 criteria that stops the search. Thus, there are $O(\log(1/\varepsilon_S))$ non-empty distance classes.

208 We use Stirling's formula to bound the volume of the Euclidean d -ball of radius 1

$$209 \quad \kappa_d = \text{Vol}(ball(1)) \in \left[\frac{\pi^{d/2}}{[d/2]!}, \frac{\pi^{d/2}}{[d/2]!} \right] = \Theta_d(d^{-(d+1)/2}) . \quad (5)$$

210 ► **Lemma 4** (Simple Bound). There are $O_d(1/\varepsilon_A^d)$ canonical cubes in class L_j .

211 **Proof.** All cubes of distance class L_j are contained in the d -ball around s with radius $2^j r$,
 212 which has the volume $\text{Vol}(ball_s(2^j r)) = \kappa_d \cdot (2^j r)^d = O_d((2^j r)^d / d^{(d+1)/2})$. Thus, it suffices
 213 to show that any one cube has side-length at least $\varepsilon_A 2^j r / (8\sqrt{d})$.

214 From the distance class partition, we have that a cube with diameter δ in class j has that
 215 all of its points have distance $\geq 2^j r/2 - \delta$ from the center s .

216 Now, having the top-down search visit a cube C with diameter δ would require the search
 217 did not terminate at its parent C' , which has diameter 2δ . Thus, 2δ was not sufficiently small
 218 for stopping, i.e. $2\delta > \varepsilon_A(\|s_i - \text{centr}(C')\| - 2\delta/2)$. Since $\text{centr}(C') \in C$, its distance from
 219 s_i is at least $2^j r/2 - \delta$. Hence, $2\delta > \varepsilon_A(2^j r/2 - 2\delta)$, which implies that $\delta > \frac{\varepsilon_A}{1+\varepsilon_A} \cdot 2^j r/4$.

220 Thus, any cube in L_j must have diameter $\geq \varepsilon_A \cdot 2^j r/8$, and consequently side-length
 221 $\geq \varepsilon_A \cdot 2^j r/(8\sqrt{d})$. \blacktriangleleft

222 Thus, the lemma yields a running time bound and, consequently, a result size bound. In
 223 the full paper, we show that this bound can be improved by one $(1/\varepsilon_A)$ -factor.

224 We summarize our results thus far before discussing how to assemble the Approximate
 225 Voronoi Diagram from the ε_A -approximations of the cores.

226 **► Theorem 5.** *Let $\mathcal{R} \subseteq \mathbb{R}^d$ be a region that is the intersection of k bisectors of $O(1/\varepsilon_S)$ -
 227 fatness, s its center, and $\varepsilon_A \in (0, \varepsilon_S)$. One can compute a set L of $O_d(\log(1/\varepsilon_S)/\varepsilon_A^{d-1})$
 228 canonical cubes that ε_A -approximates (\mathcal{R}, s) . Time is an $O(d \cdot k)$ -factor over the size bound.*

229 Our lower bound in [Theorem 7](#) will show that $\Omega_d\left(\frac{\log(1/\varepsilon)}{\varepsilon^{d-1}}\right)$ cubes are required, if $\varepsilon \ll 1/d^3$.

230 3.1 Assembling the Approximate Diagram from Cubes

231 In this section, we combine the ε_A -approximations of each of the regions $\text{core}(B_i)$ to construct
 232 an ε -AMWVD, where $\varepsilon = (1 + \varepsilon_S)(1 + \varepsilon_A) - 1$. For each $1 \leq i < n$, we construct the
 233 ε_A -approximate cubes for $(\text{core}(B_i), s_i)$ using [Theorem 5](#). Each cube in the ε_A -approximation
 234 of $(\text{core}(B_i), s_i)$ is given the label i . We collect all cubes for all labels $1 \leq i < n$ in a list. For
 235 $i = n$, we construct a canonical cube that contains all other canonical cubes for $1 \leq i < n$,
 236 and give this canonical cube the label n and also add it to the list. (This cube will be at the
 237 root of the compressed QuadTree.)

238 Sort the list of canonical cubes by their z -order. To remove duplicate cubes, iterate over
 239 the sorted list and keep only the cube with the minimum label (from those that are identical
 240 cubes). Construct a compressed QuadTree from this set of canonical cubes using, say, the
 241 Divide&Conquer approach (see Lemma 2.11 in [13]). The leaves of the compressed QuadTree
 242 induces a subdivision of \mathbb{R}^d , where each cell in the subdivision is either a canonical cube, or
 243 the set difference of at most 2^d canonical cubes.

244 Finally, we label all cells in the compressed QuadTree as follows. The cubes that are
 245 from the the sorted list have their initial label, and the root has initial label n . Starting
 246 at the root, if a child is unlabeled, or the child has larger label than its parent, then the
 247 child replaces its label with its parent's label. We repeat this process for all nodes in the
 248 compressed QuadTree in top-down fashion, say in a DFS traversal. This completes the
 249 construction of the approximate Voronoi Diagram.

250 To answer approximate (weighted) nearest-neighbor queries, given a query point $q \in \mathbb{R}^d$,
 251 we search our QuadTree for the smallest canonical cube containing q . The weighted nearest-
 252 neighbor of q is the site with index equal to the label stored at this node. Recall that
 253 point-location time in a compressed QuadTree is $O(d \log N)$ where N is the number of cubes
 254 in the tree.

255 Next, we prove the correctness of our proposed construction. When querying with a point
 256 q , we have two cases: Either the label returned is n , or it is less than n . If the label is n , then
 257 by construction, q is in none of the ε_A -approximations of $(\text{core}(B_i), s_i)$, for any $1 \leq i < n$.
 258 Therefore, q is outside the ε_A -approximation of $\text{core}(B_i)$ for all $1 \leq i < n$, so s_n is indeed

XX:8 Approximate Multiplicatively Weighted Voronoi Diagrams with Optimal Size

259 the site with the smallest weighted distance to q , up to a factor of $(1 + \varepsilon)$. Otherwise, let the
 260 label be i , for some $1 \leq i < n$. Due to the top-down propagation, we know that there is no
 261 canonical cube in the sorted list that both, contains q and has label less than i . Therefore,
 262 q is outside the ε_A -approximations of $\text{core}(B_j)$ for all $j < i$. So q has smaller (weighted)
 263 distance to s_i than any of $\{s_1, \dots, s_i\}$, up to a factor of $(1 + \varepsilon)$. Moreover, we know that q
 264 is in the ε_A -approximation of $\text{core}(B_i)$. Therefore, up to a factor of $(1 + \varepsilon)$, q has smaller
 265 weighted distance to s_i than any of $\{s_i, \dots, s_n\}$.

266 Since the time for top-down label propagation is linear in the tree size, our construction
 267 time bound is one logarithmic factor over the size bound:

268 **► Theorem 6.** *Given $\varepsilon_S > \varepsilon_A > 0$ and a set of balls B_i for each $i < n$, one can com-
 269 pute an ε -approximate Voronoi Diagram, where $\varepsilon = (1 + \varepsilon_S)(1 + \varepsilon_A) - 1$, with total size
 270 $O_d(n \log(1/\varepsilon_S)/\varepsilon_A^{d-1})$. The construction time is $O_d\left(\log \frac{n}{\varepsilon_A} + n^{-1} \sum_i |B_i|\right)$ times the size
 271 bound. Moreover, time to locate a query-point is $O(d \log(n) + d^2 \log(1/\varepsilon_A))$.*

272 This theorem will be used as a tool in Section 5, where we improve the construction time
 273 to near-linear, using our efficient construction of a bisector coreset for the $\{B_i\}$. Note that
 274 the construction time is already quadratic in n , since $|B_i| < n$ for all i . Next, we show that
 275 the result size is optimal, up to $\Theta_d(1)$ factors.

4 A Matching Lower Bound for Diagram Size

276 In this section, we show our matching lower bound for the size of ε -AMWVDs. That is, any
 277 subdivision comprised of axis-aligned hyper-rectangles requires $\Omega_d(n \cdot \log(1/\varepsilon)/\varepsilon^{d-1})$ cells.
 278 Our MWVD instances consist of n copies of a two-site instance that are placed sufficiently
 279 far from each other. The main idea for the two-site instance is that there are $\Omega(\log 1/\varepsilon)$
 280 distinct regions of space, each of which having a ‘large’ total volume but having a geometric
 281 shape that only allows to cover a relative ‘small’ volume with any one cell. Though the basic
 282 approach is similar to the $\Omega_d(n \cdot \varepsilon/(\sqrt{d}\varepsilon)^d)$ lower bound in [4, Section 5], the difference is
 283 that that our argument addresses various sections of two Apollonian balls with curvatures
 284 $\Theta(\varepsilon)$, instead of one hyper-cylinder that is bounded by two parallel hyper-planes. This results
 285 in a bound that is stronger by a $(d^{(d-1)/2} \log \frac{1}{\varepsilon})$ -factor than the known bound for unit-weight
 286 ε -AVDs, and matches our upper bound in Theorem 5 up to $\Theta_d(1)$ -factors.

287 Though it is an intriguing problem to also settle the question of optimal complexity
 288 for unit-weight ε -AVDs, it is, unfortunately, quite unclear if one can obtain such a bound
 289 without curved MWVD bisectors. (Cf. last two paragraphs of Section 8 in [5].)

290 **► Theorem 7.** *Let $\varepsilon \in (0, 1/16d^3]$, $w_I = 1$, $w_O = (1 + \varepsilon)^2$, and $B := \text{ball}(s_I, s_O, w_O/w_I)$ be
 291 the Apollonian ball of $s_I = (-1/\sqrt{d}, \dots, -1/\sqrt{d})$ and $s_O = ((1 + \varepsilon)^2/\sqrt{d}, \dots, (1 + \varepsilon)^2/\sqrt{d})$.
 292 Any subdivision of \mathbb{R}^d in axis-aligned hyper-rectangles that is an ε -approximation of the
 293 MWVD bisector B must contain $\Omega_d(\log(1/\varepsilon)/\varepsilon^{d-1})$ cells.*

294 **Proof.** Any ε -approximation of the MWVD of B must assign the points inside $B_I :=$
 295 $\text{ball}(s_I, s_O, (1 + \varepsilon)^3)$ to site s_I and outside $B_O := \text{ball}(s_I, s_O, 1 + \varepsilon)$ to site s_O , i.e. only the
 296 points in $B_O \setminus B_I$ may be labeled with either site. Thus, any one cell c in an ε -approximation
 297 must not intersect both, B_I and $\mathbb{R}^d \setminus B_O$. Note that $B_I \subset B \subset B_O$ and the sites, as well as
 298 the centers m_I and m_O , are co-linear, i.e. on the main diagonal. From (3) and (4), we have
 299 that $t^* = 1$ and that t^* and t^\dagger have the relations
 300

$$301 \quad t_I^\dagger(1 + \varepsilon) = t^\dagger = t_O^\dagger/(1 + \varepsilon)$$

302 $t_I^*(1 + \varepsilon) = t^* = t_O^*/(1 + \varepsilon) ,$

303 which shows that their radii, i.e. $r = (t^* + t^\dagger)/2$, have relation $r_I(1 + \varepsilon) = r = r_O/(1 + \varepsilon)$.
 304 The radii are $\Theta(1/\varepsilon)$.

305 Let w.l.o.g. the t_I^* point on B_I be at the origin. Let A contain the points from the upper
 306 half-space of $B_O \setminus B_I$, where upper/lower is due to a fixed hyper-plane that contains the
 307 main diagonal. Define partition $A =: \cup_i A_i$ such that the points in A_i have a norm in range
 308 $(2^i, 2^{i+1}]$, and let A_{-1} have the points with norm ≤ 1 . We prove the following three claims
 309 in the full version of the paper.

310 \triangleright **Claim 8.** Let $A = B_O \setminus B_I$. The i -th section $A_i = \{x \in A : \|x\| \in (2^i, 2^{i+1}]\}$ has volume
 311 at least $\text{Vol}(A_i) \geq \varepsilon 2^i \cdot \kappa_{d-1} 2^{(i+1)(d-1)-1} = \Omega_d(\varepsilon 2^{di}/d^{d/2})$.

312 \triangleright **Claim 9.** Any axis-aligned hyper-rectangle c , which does not contain points from B_I , can
 313 cover a volume of at most $\text{Vol}(c \cap A_i) = O_d((\varepsilon 2^i)^d/d^{(d+1)/2})$.

314 \triangleright **Claim 10.** Let $\varepsilon \in (0, 1/d^3]$. Any axis-aligned hyper-rectangle c , which does not contain
 315 points from $\mathbb{R}^d \setminus B_O$, can cover a volume of at most $\text{Vol}(c \cap A_i) = O_d((\varepsilon 2^i)^d/d^{(d+1)/2})$,
 316 provided index $i \leq \frac{5}{4} \log_2(1/\varepsilon)$.

317 Thus, $\Omega_d\left(\frac{\varepsilon 2^{di}/d^{d/2}}{(\varepsilon 2^i)^d/d^{(d+1)/2}}\right) = \Omega_d(\sqrt{d}/\varepsilon^{d-1})$ hyper-rectangles are necessary to cover any of
 318 the $\Omega(\log 1/\varepsilon)$ many sections from A . ◀

319 **5 Approximate Cores: Computing Bisector Coresets Efficiently**

320 Next, we define the notion ε -approximation that we use for the proof (Section 5.2) of the
 321 quality guarantee for the algorithm in Section 5.1. It extends the intuitive idea that ‘large
 322 balls’ in the set B_i may not be relevant for the intersection that defines $\text{core}(B_i)$.

323 Let α -ball(i, j) denote the enlarged ball that is obtained by setting the effective weight to
 324 $w_j/\alpha w_i$ in the bisector, i.e. α -ball(i, j) = ball($s_i, s_j, \gamma_{ij}/\alpha$). For $\alpha \geq 1$, we define a relation
 325 between any two subsets $X, Y \subseteq B_i$ from the bisectors of s_i as

326
$$X \prec_\alpha Y \iff \forall (i, k) \in Y : \text{core}(X) \subseteq \alpha\text{-ball}(i, k) ,$$

327 and say for such a pair that X is an α -cover of Y . Given a subset $X \subseteq B_i$, we call the largest
 328 subset $Y \subseteq B_i$ with $X \prec_\alpha Y$ the set of balls that are α -covered by X . Further, X is called
 329 an α -cover if it covers all balls in B_i , i.e. $X \prec_\alpha B_i$, and we have

330
$$\text{core}(B_i) \subseteq \text{core}(X) \subseteq \alpha\text{-core}(B_i) := \bigcap_{(i,j) \in B_i} \alpha\text{-ball}(i, j) . \tag{6}$$

331 For example, the set of balls that are 1-covered by a singleton set $\{(i, j)\}$ contains all balls
 332 $(i, k) \in B_i$ with $\text{ball}(i, j) \subseteq \text{ball}(i, k)$. Note that $X \prec_\alpha Y$ and $Y \prec_{\alpha'} Z$ implies $X \prec_{\alpha \cdot \alpha'} Z$.
 333 Clearly, using α -covers $\{A_1, \dots, A_{n-1}\}$ of the bisectors (i.e. $A_i \prec_\alpha B_i$ for all sites s_i) turns
 334 the ε -approximation algorithm of Section 3.1 into one that computes an ε' -approximate
 335 Voronoi Diagram, with $\varepsilon' = (1 + \varepsilon)\alpha - 1$, whose running time is sensitive to $|A_i|$.

336 The goal of our next algorithm is to compute a subsets $A_i \subseteq B_i$, so that A_i is an α -cover
 337 of B_i , and A_i has constant size. Then, we apply Theorem 6 to those bisector sets $\{A_i\}$.

338 **Recap: σ -Semi-Separated Pair Decompositions with Low Weight**

339 Let $S \subseteq \mathbb{R}^d$ be a set of n points. A list of subset pairs $\mathcal{P} = \{(X_i, Y_i) : X_i, Y_i \subseteq S, X_i \cap Y_i = \emptyset\}$
 340 is called a pair decomposition if there is, for every $\{s, s'\} \in \binom{S}{2}$, a pair $(X_i, Y_i) \in \mathcal{P}$ with
 341 $|\{s, s'\} \cap X_i| = 1 = |Y_i \cap \{s, s'\}|$. The quantity $\sum_i (|X_i| + |Y_i|)$ is called the *weight* of the
 342 pair decomposition \mathcal{P} . It is well known that a pair decomposition of n points has weight
 343 $\Omega(n \log n)$. (See [13, Lemma 3.31].)

344 A pair decomposition \mathcal{P} of S is called a σ -SSPD with respect to constant $\sigma > 1$, if every
 345 point set pair $(X, Y) \in \mathcal{P}$ has the separation property

$$346 \min \left\{ \max_{x, x' \in X} \|x - x'\|_2, \max_{y, y' \in Y} \|y - y'\|_2 \right\} \cdot \sigma \leq \min_{x \in X, y \in Y} \|x - y\|_2. \quad (7)$$

347 That is, the two sets have a closest-pair distance of at least σ times the small diameter.

348 Given a set of n points from \mathbb{R}^d , a σ -SSPD with weight $w(n, d, \sigma) = O_d(d^{7d/2} \sigma^d n \log n) =$
 349 $O_D(\sigma^d n \log n)$ can be computed in deterministic $O_D(\sigma^d n + n \log n)$ time [1, Theorem 5]. For
 350 point sets with polynomially bounded spread, it is possible to improve both (deterministic)
 351 O_D -bounds to O_d -bounds with a QuadTree based pair decomposition, using [2, Lemma 2.8].

352 The efficiency of our coreset construction stems from low weight SSPDs. We use the
 353 SSPD separation in terms of the radius of the two sets, which increases σ by a factor of two.

354 **5.1 Computing Approximate Cores: SSPDs and Conic Space Partitions**

355 Let $\beta, \varepsilon_C > 0$ and $\sigma \geq 2$ be constants, which we calibrate in Section 5.2. A β -cone around
 356 s_i is an angular domain of the spherical coordinate system around s_i . Each of its $(d - 1)$
 357 angular dimensions is partitioned into intervals of at most 2β radians. For each s_i , we assign
 358 each β -cone a unique array index j , where $j = O_d(1/\beta^{d-1})$. E.g. a rotation of at most β
 359 radians suffices to rotate any point in the cone onto the cone's central ray.

360 Let \mathcal{P} be a σ -SSPD of the input sites S . For a pair $(L, H) \in \mathcal{P}$, we call L the ‘light set’
 361 and H the ‘heavy set’ if s_ℓ is the site with maximum index in L , s_h is the site with the
 362 maximum index in H , and $\ell < h$.

363 Our algorithm maintains the following structure: For each site $s_i \in S$, and for each
 364 β -cone around s_i with array index j , the data structure stores a set of partner sites A_{ij} . Our
 365 algorithm populates the structure in three passes. In our first pass, for each $(L, H) \in \mathcal{P}$, we
 366 reduce the size of H to a subset H' . In our second pass, we iterate over \mathcal{P} to initialize each
 367 of the sets A_{ij} . Finally, the sets are populated in the third pass.

368 In our first pass, for each $(L, H) \in \mathcal{P}$, we construct a subset H' of H . If the diameter of
 369 H is at most the diameter of L , we set $H' := \emptyset$. If the diameter of H is larger than the
 370 diameter of L , we construct H' as follows. Let $s_\ell \in L$ with ℓ maximal. For the j^{th} cone
 371 around s_ℓ , we let the sites of H contained in this cone be $C_{\ell j}$. We use the following function:

```

372 Scan-Cone-Sites( $i, C, \varepsilon_C$ ):
373   Let  $C' := \emptyset$ ,  $a = \min\{t_{ij}^* : s_j \in C\}$ , and  $b = \min\{t_{ij}^\dagger : s_j \in C\}$ .
374   Let  $I_k = (x_k, x_{k+1}]$ , with length  $a\varepsilon_C/2$  and  $x_1 = a$ , cover  $[a, b]$ .
375   Every interval  $I_k$  holds one pointer.
376   FOR  $s_j \in C$  DO
377     Compute the index  $k$  with  $t_{ij}^* \in I_k$ .
378     If diameter  $(t_{ij}^* + t_{ij}^\dagger)$  is smaller than that of  $I_k$ 's reference,
379       then set  $I_k$ 's pointer on  $s_j$ .
380   FOR interval  $I_k$  DO
381     Add the kept bisector to result set  $C'$ .
382   return  $C'$ 
383

```

385 We select for the j^{th} cone a subset by setting $C'_{\ell_j} := \text{Scan-Cone-Sites}(\ell, C_{\ell_j}, \varepsilon_C)$ and define
 386 $H' = \cup_j C'_{\ell_j}$. This completes the construction of H' .

387 In our second pass, we initialize each cone of each site in our structure to store an
 388 interval $[a, b]$. We iterate over all pairs $(L, H) \in \mathcal{P}$ and all $s_i \in L \cup H$, and store for j^{th}
 389 cone of s_i , a variable a equal to the minimum value of a t_{ik}^* , and a variable b equal to the
 390 minimum value of a t_{ik}^\dagger . This minimum is taken over all sites $s_k \in H' \cup \{s_\ell, s_h\}$ that are
 391 in the j^{th} cone of s_i and have $k > i$. This gives us the interval $[a, b]$. After the pass over
 392 \mathcal{P} is completed, we iterate over each cone of each site and partition the interval $[a, b]$ into
 393 disjoint intervals $I_k = (x_k, x_{k+1}]$ of length $a\varepsilon_C/2$ that cover $[a, b]$, i.e. $x_{k+1} - x_k = a\varepsilon_C/2$
 394 and $x_1 = a$.

395 In our third pass, we populate the sets A_{ij} based on the intervals $\{I_k\}$ of the j^{th} cone
 396 of s_i . We iterate over all pairs $(L, H) \in \mathcal{P}$ and maintain a reference from I_k to the site that
 397 realized a minimum diameter. For $s_i \in L \cup H$, and for the j^{th} cone around s_i , we let the sites
 398 $s_m \in H' \cup \{s_\ell, s_h\}$ with $m > i$ that are contained in this cone be C_{ij} . For each $s_m \in C_{ij}$, we
 399 locate the interval I_k of the cone that contains t_{im}^* and compare the diameter of $\text{ball}(i, m)$
 400 with the smallest diameter of I_k that we have encountered so far. If the diameter of $\text{ball}(i, m)$
 401 is smaller, we set s_m to be the site of I_k realizing the minimum diameter. After the pass
 402 over all pairs is completed, for the j^{th} cone of site s_i , and for all intervals I_k , we add the site
 403 that realized the minimum diameter for I_k into the set A_{ij} . This completes our three passes
 404 that construct the cone sets. Finally, we set $A_i = \cup_j A_{ij}$, and then apply [Theorem 6](#) to the
 405 set of balls A_i .

406 In the next section, we show that A_i is an α -cover of B_i . The algorithm's runtime bound
 407 $O_d(w(n, d, \sigma) \cdot m/\beta^{d-1})$ will follow from weight $w(n, d, \sigma)$ of a σ -SSPD, the number of β -cones
 408 in the partitions of \mathbb{R}^d , and the maximum number m of sites in the sets A_{ij} .

409 5.2 Correctness: Choosing Sufficient β , σ , and ε_C

410 Our $(1 + \varepsilon)$ bound consists of seven components for each of the convex cores. The components
 411 use the target approximation ε_A for the Adaptive Refinement in [Section 3](#), an ε_S that scales
 412 half-space bisectors to sufficiently large balls (see [Section 2.1](#)), an ε_C that is the tolerance for
 413 selecting a small set of sites per β -cone, an ε_T that virtually translates sites along a ray from
 414 another site, and ε_R that virtually rotate a site's partner (cf. [Figure 2](#)).

415 For prescribed $\varepsilon > 0$, we set the components such that

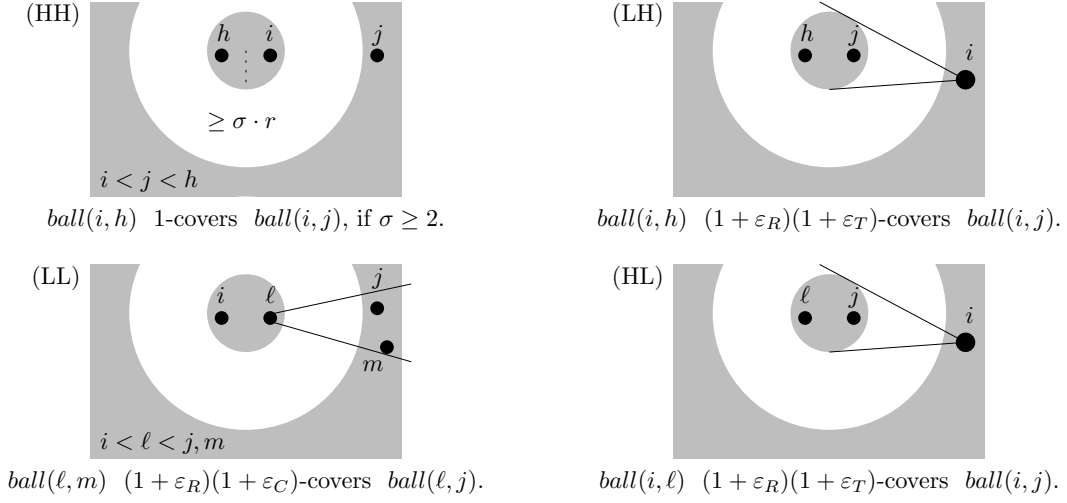
$$416 (1 + \varepsilon_A)(1 + \varepsilon_S)(1 + \varepsilon_T)(1 + \varepsilon_R)^2(1 + \varepsilon_C)^2 \leq 1 + \varepsilon \tag{8}$$

$$417 \max\{\varepsilon_R, \varepsilon_T, \varepsilon_C\} < \varepsilon_S, \tag{9}$$

418 where the last inequality is *strict* to accommodate [Lemma 13](#). For example, we can set
 419 $\varepsilon_S = \varepsilon/8$ and $\varepsilon_A = \varepsilon_C = \varepsilon_R = \varepsilon_T = \varepsilon/16$.

420 This section shows $\text{core}(A_i) \subseteq \left(\frac{1+\varepsilon}{1+\varepsilon_A}\right)\text{-core}(B_i)$ and consequently the approximation
 421 bound of our approach. Recall from [Section 2.1](#) that all bisectors in B_i have $w_j/w_i \geq 1 + \varepsilon_S$.

422 To show inclusion properties, we will use the following parametrization of balls in B_i :
 423 Consider a fixed ray q , say the x -axis, that emanates from the origin s_i , having $w_i = 1$.
 424 Ignoring the input instance S briefly, any pair (s, w) of a point s on q and a real $w > 1$ defines
 425 a ball, with respective two points on the x -axis of distance $t^*, t^\dagger > 0$. It is convenient to use
 426 parametrization (t^*, t^\dagger) , instead of (s, w) , to describe this ball: If input sites s_j and s_k are on
 427 the same ray q , then $\text{ball}(i, j) \subseteq \text{ball}(i, k) \Leftrightarrow t_{ij}^* \leq t_{ik}^* \wedge t_{ij}^\dagger \leq t_{ik}^\dagger$. It is noteworthy that
 428 both inequalities can be decided without square-root computations (cf. [Eq. \(3\)](#) and [\(4\)](#)).



437 ■ **Figure 2** Cases (HH), (LH), (HL), and (LL), for covering an absent ball $(i, j) \in B_i \setminus A_i$.

429 To show that every $(i, j) \in B_i \setminus A_i$ is α -covered, the main idea is to consider the pair
 430 $(L, H) \in \mathcal{P}$ that separates it to observe that at least one bisector that α -covers (i, j) is
 431 contained in A_i . There are four cases for an absent bisector (i, j) : (LL) $s_i \in L$ and L
 432 has smaller diameter, (LH) $s_i \in L$ and H has smaller diameter, (HL) $s_i \in H$ and L
 433 has smaller diameter, and (HH) $s_i \in H$ and H has smaller diameter. We use at most
 434 three affine transformations to bound each case. See Figure 2. The bound for (LL) is
 435 $\alpha = (1 + \varepsilon_R)^2(1 + \varepsilon_C)^2(1 + \varepsilon_T)$, the bound for (LH) is $\alpha = (1 + \varepsilon_R)^2(1 + \varepsilon_T)(1 + \varepsilon_C)$,
 436 the bound for (HL) is $\alpha = (1 + \varepsilon_R)^2(1 + \varepsilon_T)(1 + \varepsilon_C)$, and the bound for (HH) is $\alpha = (1 + \varepsilon_R)(1 + \varepsilon_C)$.

438 We start by showing an observation about pair decompositions. A cluster of points H
 439 that is, relative to its diameter, far from a given point s_i can be rotated with a small angle
 440 onto a common ray q , from s_i through an arbitrary point s_h from the cluster.

441 ► **Observation 11** (Distant clusters). *Let angle $\beta \in (0, 1]$, $s_i \in S$, c and r be the center and
 442 radius of the minimum enclosing ball of $H \subseteq S \setminus \{s_i\}$, $\sigma := \|s_i - c\|/r > 0$, and $s_h \in H$. If
 443 $\sigma \geq 2/\beta$, then $\angle s' s_i s_h \in [0, \beta]$ for all $s' \in H$.*

444 **Proof.** Since $\frac{r}{r\sigma} = \tan \frac{\beta}{2} = \frac{\sin \beta}{1 + \cos \beta} \leq \frac{\beta}{1 + (1 - \beta^2)} = \frac{1}{2/\beta - \beta}$ and $\beta \geq 0$, any $\sigma \geq 2/\beta$ suffices. ◀

445 This observation motivates our main lemma that analyzes the enlargement of a ball from
 446 B_i that is required to contain the ball that is obtained from a small rotation around s_i .

447 ► **Lemma 12** (Rotations at s_i). *If $\beta = \angle s_j s_i s_k \in [0, 1]$ and $[t_{ij}^*, t_{ij}^\dagger] = [t_{ik}^*, t_{ik}^\dagger]$, then
 448 $ball(i, j) \subseteq \alpha$ -ball(i, k) for all $\alpha \geq 1 + \beta^2/2$.*

449 Note that this bound also applies to rotations of s_i on s_j around s_k for $k > i, j$, i.e.
 450 if $[t_{ik}^*, t_{ik}^\dagger] = [t_{jk}^*, t_{jk}^\dagger]$ and $\beta = \angle s_i s_k s_j$ is small, then $B \subseteq \alpha$ -ball(j, k), where B is the
 451 translation of $ball(i, k)$ with the vector $\overrightarrow{s_i s_j}$.

452 So far we showed that choosing a cone angle $\beta = \sqrt{2\varepsilon_R}$ and $\sigma \geq 2/\sqrt{2\varepsilon_R}$ satisfies the
 453 $(1 + \varepsilon_R)$ -factors for rotations in all cases (i.e. LL, LH, HL, and HH). Next we show that
 454 translations of sites in the low diameter set have a $(1 + \varepsilon_T)$ -bound, for sufficiently large σ .

455 ▶ **Lemma 13** (Translations). *Let p and q be on a common ray from s , $\|s-p\| < \|s-q\|$, $\varepsilon_T \in$
 456 $(0, \varepsilon_S)$, point $m := (p+q)\frac{1}{2}$, $r := \|m-p\|$. If $1+\varepsilon_T < \gamma$, then we have that $\|s-m\| \geq \sigma r$ implies
 457 that $t^*(s, q, \gamma) \leq t^*\left(s, p, \frac{\gamma}{1+\varepsilon_T}\right)$ and $t^\dagger(s, q, \gamma) \leq t^\dagger\left(s, p, \frac{\gamma}{1+\varepsilon_T}\right)$, for all $\sigma \geq 1 + 2/\varepsilon_T$.
 458 This also implies that $t^*(q, s, \gamma) \leq t^*\left(p, s, \frac{\gamma}{1+\varepsilon_T}\right)$ and $t^\dagger(q, s, \gamma) \leq t^\dagger\left(p, s, \frac{\gamma}{1+\varepsilon_T}\right)$.*

459 The first translation property is used for the cases where H has smaller diameter and the
 460 second for the cases where L has smaller diameter. One may think of the above discussion as
 461 a means to virtually place all sites in the low diameter set at the same spatial point with two
 462 transformations. We now show that partners of s_i with lower weight than other partners,
 463 transformed to the same location, can be ignored in an α -cover (e.g. [Figure 2](#) LH and HL).

464 ▶ **Observation 14** (Weight Monotonicity). *If $1 < \gamma \leq \gamma'$, then $\text{ball}(p, q, \gamma') \subseteq \text{ball}(p, q, \gamma)$.*

465 **Proof.** We give the, slightly more technical, argument for $t^\dagger(p, q, \gamma') \leq t^\dagger(p, q, \gamma)$. This holds
 466 iff $\frac{\|p-q\|}{\gamma'-1} \leq \frac{\|p-q\|}{\gamma-1}$, which holds iff $\gamma' - 1 \geq \gamma - 1$, since $\gamma - 1 \neq 0 \neq \gamma' - 1$. ◀

467 Thus, for case (LH) and (HL) it suffices that s_i scans s_h and s_ℓ , respectively. (They are
 468 member of $H' \cup \{s_\ell\} \cup \{s_h\}$ and checked by algorithm when pair (L, H) is considered.) It
 469 remains to prove the $(1 + \varepsilon_C)$ factor in the approximations of **Scan-Cone-Sites**.

470 ▶ **Lemma 15** (Constant per cone). *Let $\{s_2, \dots, s_n\}$ be on a common ray from s_1 , $w_i/w_1 \geq$
 471 $1 + \varepsilon_S$, and $\varepsilon_S > \varepsilon_C > 0$. Computing a $C_1 \subseteq B_1$ of size $O(1/\varepsilon_C \varepsilon_S)$, with $C_1 \prec_{(1+\varepsilon_C)} B_1$,
 472 takes $O(n)$ time.*

473 Thus, selecting at most $m = O(1/\varepsilon_C^2)$ sites per cone introduces only a factor of $(1 + \varepsilon_C)$.
 474 This completes the argument for all four cases, and we have $\text{core}(A_i) \subseteq \frac{1+\varepsilon}{1+\varepsilon_A}\text{-core}(B_i)$. Taking
 475 $\sigma = 1 + 2/\varepsilon_T$, $\beta = \sqrt{2\varepsilon_R}$, and $m = O(\varepsilon_C^{-2})$, the coresets construction time $O_d(w(n, d, \sigma) \cdot$
 476 $m/\beta^{d-1}) = O_D((\varepsilon^{-d} n \log n) \cdot \varepsilon^{-2} \varepsilon^{-(d-1)/2}) = O_D(n \log(n)/\varepsilon^{3(d+1)/2})$. We summarize:

477 ▶ **Theorem 16.** *The approximation algorithm computes, for each $1 \leq i < n$, a subset $A_i \subseteq B_i$
 478 with $\text{core}(A_i) \subseteq \frac{1+\varepsilon}{1+\varepsilon_A}\text{-core}(B_i)$ and $|A_i| = O_d(1/\varepsilon^{(d+3)/2})$ in $O_D(n \log(n)/\varepsilon^{3(d+1)/2})$ time.*

479 We are now ready to show our main result.

480 ▶ **Corollary 17.** *For any $\varepsilon > 0$, one can compute an ε -AMWVD of size $O_d(n \log(1/\varepsilon)/\varepsilon^{d-1})$.
 481 The construction time is $O_D(\log(n)/\varepsilon^{(d+5)/2})$ times the output size.*

482 *The query time of the search structure is $O(d \log(n) + d^2 \log(1/\varepsilon))$.*

483 **Proof.** Applying [Theorem 6](#) on the bisector coresets that are obtained from [Theorem 16](#), the
 484 construction time of the ε -AMWVD is a factor $O_d(|A_i| + \log(n/\varepsilon)) = O_d(\log(n/\varepsilon)/\varepsilon^{(d+3)/2})$
 485 over the output size bound. Hence, construction time is dominated by computing the bisector
 486 coresets, taking a factor $O_D\left(\frac{n \log(n)/\varepsilon^{3(d+1)/2}}{n \log(1/\varepsilon)/\varepsilon^{d-1}}\right) = O_D(\varepsilon^{-(d+5)/2} \log(n)/\log(1/\varepsilon))$ over the
 487 output size bound. ◀

488 — References

- 489 1 Mohammad Ali Abam, Mark de Berg, Mohammad Farshi, Joachim Gudmundsson, and Michiel
490 H. M. Smid. Geometric spanners for weighted point sets. *Algorithmica*, 61(1):207–225, 2011.
491 doi:[10.1007/s00453-010-9465-2](https://doi.org/10.1007/s00453-010-9465-2).
- 492 2 Mohammad Ali Abam and Sariel Har-Peled. New constructions of SSPDs and their applications.
493 *Comput. Geom.*, 45(5-6):200–214, 2012. doi:[10.1016/j.comgeo.2011.12.003](https://doi.org/10.1016/j.comgeo.2011.12.003).
- 494 3 Boris Aronov, Gali Bar-On, and Matthew J. Katz. Resolving SINR queries in a dynamic
495 setting. *SIAM J. Comput.*, 49(6):1271–1290, 2020. doi:[10.1137/19M128733X](https://doi.org/10.1137/19M128733X).
- 496 4 Sunil Arya and Theocharis Malamatos. Linear-size approximate Voronoi diagrams. In *Proc.*
497 *13th ACM-SIAM Symposium on Discrete Algorithms (SODA'02)*, pages 147–155, 2002. URL:
498 <http://dl.acm.org/citation.cfm?id=545381.545400>.
- 499 5 Sunil Arya, Theocharis Malamatos, and David M. Mount. Space-time tradeoffs for approximate
500 nearest neighbor searching. *J. ACM*, 57(1):1:1–1:54, 2009. doi:[10.1145/1613676.1613677](https://doi.org/10.1145/1613676.1613677).
- 501 6 Franz Aurenhammer. The one-dimensional weighted Voronoi diagram. *Information Processing*
502 *Letters*, 22(3):119–123, 1986. URL: [https://www.sciencedirect.com/science/article/pii/](https://www.sciencedirect.com/science/article/pii/0020019086900554)
503 [0020019086900554](https://www.sciencedirect.com/science/article/pii/0020019086900554), doi:[https://doi.org/10.1016/0020-0190\(86\)90055-4](https://doi.org/10.1016/0020-0190(86)90055-4).
- 504 7 Franz Aurenhammer and Herbert Edelsbrunner. An optimal algorithm for constructing
505 the weighted Voronoi diagram in the plane. *Pattern Recognit.*, 17(2):251–257, 1984. doi:
506 [10.1016/0031-3203\(84\)90064-5](https://doi.org/10.1016/0031-3203(84)90064-5).
- 507 8 Franz Aurenhammer, Rolf Klein, and Der-Tsai Lee. *Voronoi Diagrams and Delaunay Triangu-*
508 *lations*. World Scientific, 2013. doi:[10.1142/8685](https://doi.org/10.1142/8685).
- 509 9 Bernard Chazelle. Filtering search: A new approach to query-answering. *SIAM J. Comput.*,
510 15(3):703–724, 1986. doi:[10.1137/0215051](https://doi.org/10.1137/0215051).
- 511 10 Mark de Berg, Otfried Cheong, Marc J. van Kreveld, and Mark H. Overmars. *Computational*
512 *geometry: algorithms and applications, 3rd Edition*. Springer, 2008. URL: [https://www.](https://www.worldcat.org/oclc/227584184)
513 [worldcat.org/oclc/227584184](https://www.worldcat.org/oclc/227584184).
- 514 11 Chenglin Fan and Benjamin Raichel. Linear expected complexity for directional and mul-
515 tiplicative Voronoi diagrams. In *Proc. 28th European Symposium on Algorithms (ESA'20)*,
516 pages 45:1–45:18, 2020. doi:[10.4230/LIPIcs.ESA.2020.45](https://doi.org/10.4230/LIPIcs.ESA.2020.45).
- 517 12 Sariel Har-Peled. A replacement for Voronoi diagrams of near linear size. In *Proc. 42nd*
518 *Symposium on Foundations of Computer Science (FOCS'01)*, pages 94–103, 2001. doi:
519 [10.1109/SFCS.2001.959884](https://doi.org/10.1109/SFCS.2001.959884).
- 520 13 Sariel Har-Peled. *Geometric approximation algorithms*. Number 173 in Mathematical Surveys
521 and Monographs. American Mathematical Society, 2011.
- 522 14 Sariel Har-Peled, Piotr Indyk, and Rajeev Motwani. Approximate nearest neighbor: Towards
523 removing the curse of dimensionality. *Theory Comput.*, 8(1):321–350, 2012. doi:[10.4086/toc.](https://doi.org/10.4086/toc.2012.v008a014)
524 [2012.v008a014](https://doi.org/10.4086/toc.2012.v008a014).
- 525 15 Sariel Har-Peled and Nirman Kumar. Approximating minimization diagrams and generalized
526 proximity search. *SIAM J. Comput.*, 44(4):944–974, 2015. doi:[10.1137/140959067](https://doi.org/10.1137/140959067).
- 527 16 Sariel Har-Peled and Benjamin Raichel. On the complexity of randomly weighted multi-
528 plicative Voronoi diagrams. *Discret. Comput. Geom.*, 53(3):547–568, 2015. doi:[10.1007/](https://doi.org/10.1007/s00454-015-9675-0)
529 [s00454-015-9675-0](https://doi.org/10.1007/s00454-015-9675-0).
- 530 17 Martin Held and Stefan de Lorenzo. An efficient, practical algorithm and implementation for
531 computing multiplicatively weighted Voronoi diagrams. In *Proc. 28th European Symposium*
532 *on Algorithms (ESA'20)*, pages 56:1–56:15, 2020. doi:[10.4230/LIPIcs.ESA.2020.56](https://doi.org/10.4230/LIPIcs.ESA.2020.56).
- 533 18 Yogish Sabharwal, Nishant Sharma, and Sandeep Sen. Nearest neighbors search using point
534 location in balls with applications to approximate Voronoi decompositions. *J. Comput. Syst.*
535 *Sci.*, 72(6):955–977, 2006. doi:[10.1016/j.jcss.2006.01.007](https://doi.org/10.1016/j.jcss.2006.01.007).